

ELECTROMAGNETIC TORQUE RIPPLES AND DYNAMIC BEHAVIORS OF BPM MOTORS

Petrică TARAȘ, Tiberiu TUDORACHE, Virgiliu FIREȚEANU

*POLITEHNICA University of Bucharest/Faculty of Electrical Engineering/
EPM_NM Laboratory, Bucharest, Romania
petrica_taras@amotion.pub.ro*

Abstract – This paper deals with the finite element based numerical analysis of DC BPM motor with the aim of reducing the electromagnetic torque ripples, one of the major source of vibration and acoustic noise. The analysis is focused first on the computation of the cogging torque of the motor and then on the command circuit arrangement, which has a major influence on the electromagnetic torque oscillations.

The numerical investigation using a field - circuit - motion coupling shows that the DC voltage drive strategy based on three switches entails higher torque ripples than a drive system using six switches.

Finally the electromagnetic torque oscillations are studied during the no-load start-up of the motor as well as after applying a load torque.

Keywords: brushless dc motor, finite element model, electromagnetic torque oscillations.

1. INTRODUCTION

The electronic commutation DC motor with permanent magnets, known also by the denomination BPM motor, represents a serious competitor to the AC and DC electric drives low power applications e.g. in computers, automotive industry etc. The efficient design and optimization of such a drive system calls for powerful numerical analysis of field - circuit – motion type, able to take into account complex geometries, magnetic saturation, electric supply of motor coils, etc. One of the important challenges of BPM motors is the attenuation of vibration and acoustic noise level.

The main sources of vibration and acoustic noise of the BPM motors are the electromagnetic torque ripples and the unbalanced radial forces. A strongly oscillating electromagnetic torque of the motor gives rises to speed oscillations, while an important unbalanced radial force leads to mechanical stress of the motor bearings and structural vibrations.

2. FINITE ELEMENT MODEL OF BPM MOTOR

The electromagnetic field in BPM motors without solid conductor regions is governed by the differential equation:

$$\text{curl} [(1/\mu) \text{curl} \mathbf{A}] = \mathbf{J} + \text{curl} \mathbf{H}_c \quad (1)$$

where μ is the magnetic permeability, $\mathbf{A}(\mathbf{r}, t)$ the magnetic vector potential is the unknown state variable, $\mathbf{J}(\mathbf{r}, t)$ is the current density in the coil regions and $\mathbf{H}_c(\mathbf{r})$ is the coercitive field of the magnets.

In the plane 2D models in the stator cartesian coordinate system (x, y, z) , Fig. 1, which is the case of investigations in this paper the vectors $\mathbf{J}(x,y,t)$ and $\mathbf{A}(x,y,t)$ have normal orientation with respect the plane (x, y) , while the vector $\mathbf{H}_c(x,y,t)$ is contained in it. The quantity \mathbf{H}_c is a computation date defined by the magnet properties, but the current density \mathbf{J} is in many cases another unknown of the model. This quantity is connected with the computation data that is the voltage of the BPM supply source by the equations of the circuit model attached to the field model.

This study considers a 6-pole 9-slot BPM motor with outer rotor, whose geometry, mesh and wye connected stator winding system are presented in Figures 1 - 3.

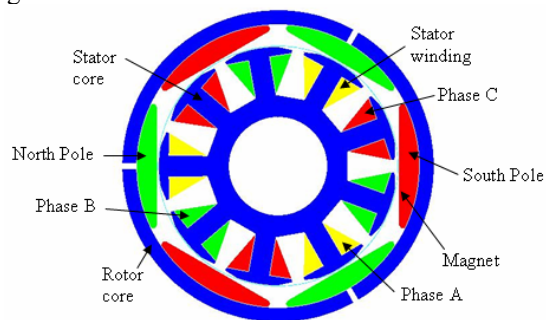


Figure 1. Electromagnetic field computation domain

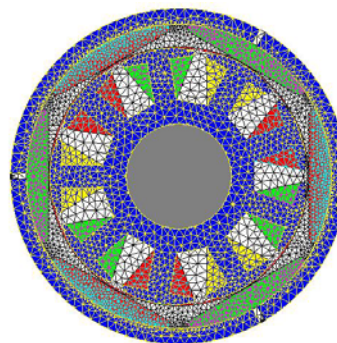


Figure 2. Mesh of the computation domain

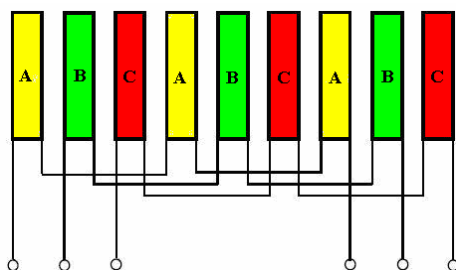


Figure 3. Winding of the studied BPM

3. COGGING TORQUE EVALUATION

The ripples of the cogging torque are the result of the variation of the magnetic reluctance of airgap between the stator and rotor armatures. Since the magnetic configuration of the motor depends on the relative position stator – rotor, the space configuration of the primary magnetic field generated by the magnets with respect the rotor is different from one rotor position to another.

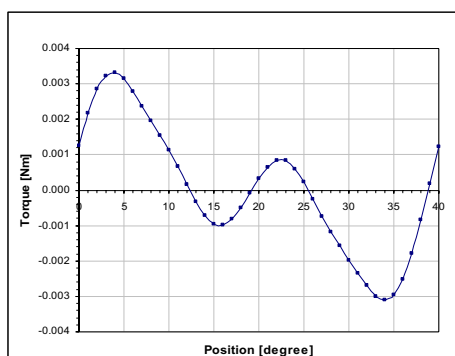


Figure 4. Cogging torque of the studied BPM motor; rotation over a tooth step, 40 mechanical degrees

The evaluation of the cogging torque is the result of a parameterized analysis based on the finite element model of the magnetostatic field generated exclusively by the motor magnets, the parameter being the relative angular position of the rotor with respect the stator. The results presented in Fig. 4 are related to the angular period of the magnetic field - 40 degrees, corresponding to a tooth pole pitch. The peak-to-peak value of the cogging torque is about 6.426 mNm.

4. ELECTROMAGNETIC TORQUE EVALUATION FOR DIFFERENT MOTOR SUPPLY SCHEMES

4.1. Motor supplied by a three-switch commutator

The simplest configuration of the studied BMP motor supply by a DC voltage source, V, Fig. 5, is an unidirectional three-phase arrangement, with only

three power switches, S1, S2 and S3. The components V1, V2 and V3 of the circuit model are set here to take in account the voltage drop on the real power silicon devices in direct conduction.

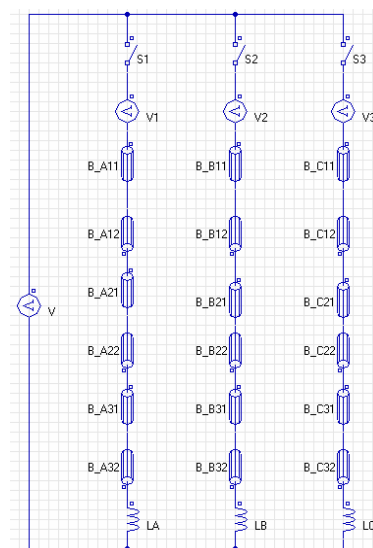


Figure 5. Circuit model with three switches

The components B_A11 ... B_A32, B_B11 ... B_B32, B_C11 ... B_C32 are of stranded coil conductor type, which take into account the active section of the conductors in the stator slots.

The end winding sections are taken into account using the LA, LB and LC inductor components.

The evaluation of the electromagnetic torque supposes a numerical simulation of magnetic transient type at imposed rotor speed. The following data were considered: DC voltage 12 V; rotor speed 1000 rpm, 13 turns per coil, one coil per tooth. The solution of the magnetic field generated by the rotor magnets and the currents in the stator coils is of type step by step in time domain, the time step being 0.2 ms

The switches are controlled according to the diagram presented in Figure 6. The variations of the electromotive force (emf) and magnetic flux quantities over a full electrical cycle are used to obtain the switches control diagram.

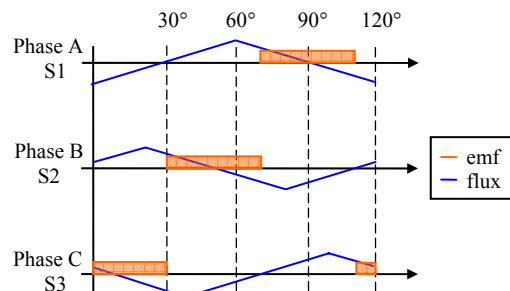


Figure 6. Control diagram, three switches

When the coils of one phase are aligned with the axis of a magnet, the flux has a maximum or minimum value, according to magnets polarity. Between the minimum and maximum values we suppose a linear variation of the flux; so, according to Faraday's law, the emf is constant.

The important oscillations of the electromagnetic torque, Fig. 7, represent 134.6 % of the mean torque value, whose value is 1.36 Nm. Due to the high electromagnetic torque oscillations, this circuit arrangement is applicable only for cheap applications, where the standards related to the acoustic noise emission are not so restrictive.

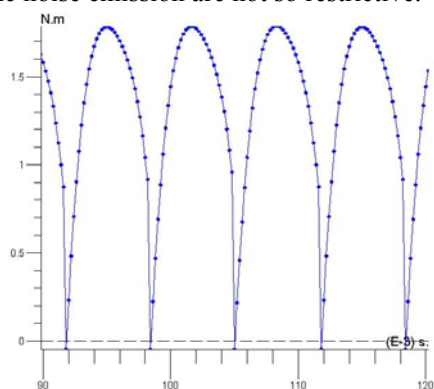


Figure 7. Electromagnetic torque oscillations; three switches, speed 1000 rpm

4.2. Motor supplied by a six-switch commutator

The classical circuit arrangement used for the motion control of the BPM motor consists of six switches, three of them conducting at any time instant, Fig. 8.

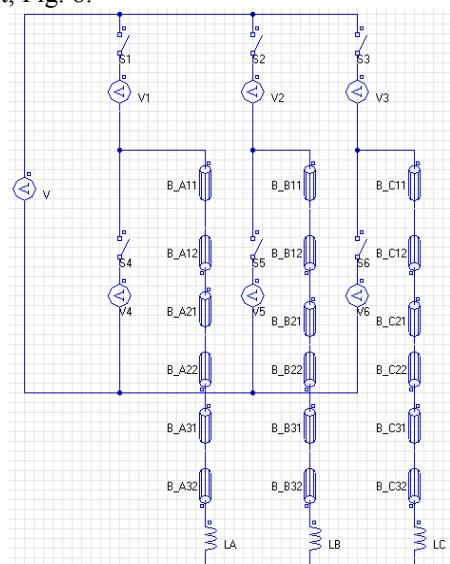


Figure 8. Circuit model with six switches

The motor control is based on the diagram presented in Figure 9.

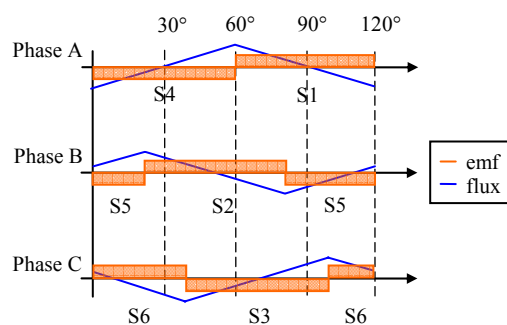


Figure 9. Control diagram, six switches

The electromagnetic torque oscillations with respect to the mean value that is 1.27 Nm, Fig. 10, are far smaller than in the case of three-switch arrangement, the peak-to-peak relative value being of only 19%. The wave of phase A current of the motor is presented in Fig. 11.

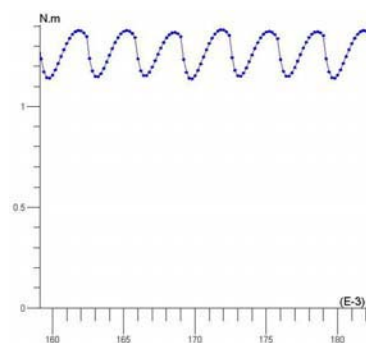


Figure 10. Electromagnetic torque oscillations; six switches, speed 1000 rpm

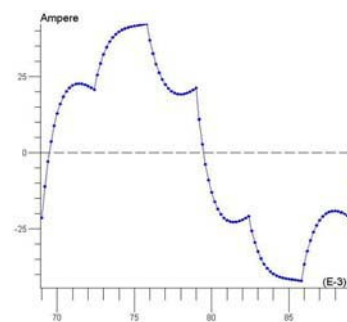


Figure 11. Phase A current; six switches, speed 1000 rpm

4.3. Motor supplied by sinusoidal currents

Another supply version supposes sine-wave currents of the three-phase winding, the circuit model of the motor being represented in Fig. 12. The numerical results obtained for 50 A peak value of phase current lead to electromagnetic torque oscillations smaller than in the previous two cases, Fig. 13. The peak-to-peak relative value in this case

is only 2 %. In this case, a study for the reduction of cogging torque becomes useful, since this component of the electromagnetic torque oscillations starts to be non-negligible.

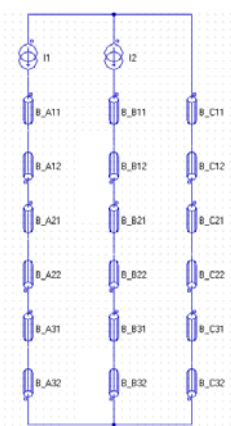


Figure 12. Circuit model with sine-wave phase currents supply

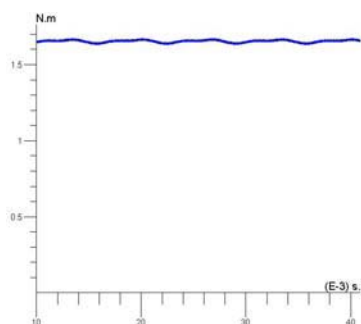


Figure 13. Electromagnetic torque oscillations; sine-wave phase currents, speed 1000 rpm

4.4. Motor supplied by a PWM voltage inverter

The simulation of the motor behavior supplied by a 6 switches inverter of PWM type, interposed between the DC voltage supply and the motor winding leads to the result presented in Figure 14.

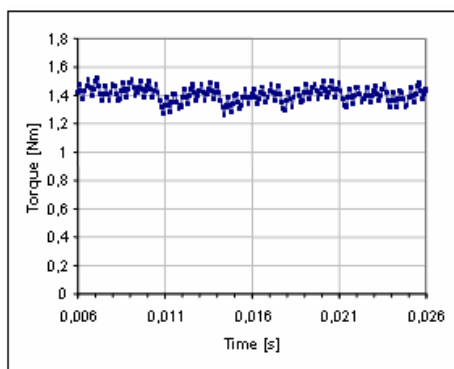


Figure 14. Electromagnetic torque oscillations; PWM supply, speed 1000 rpm

The current on phase A of the motor is presented in Figure 15. The switching frequency is 1 kHz and the magnitude modulation factor is 0.67. Unlike the previous simulations, in this case inductance of 0.1 mH/phase that plays a filtering role is series connected with the motor windings. The torque oscillations are smaller in this case, only 9.86 %, than in the cases studied in sections 5.1 and 5.2, but larger than in the case of sinusoidal current supply, section 5.3.

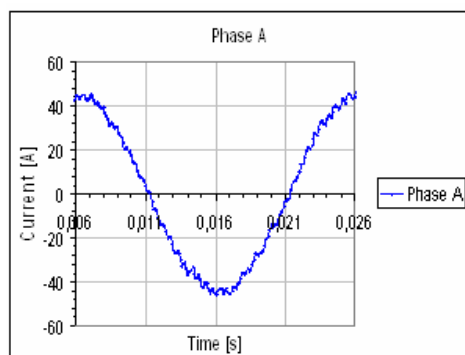


Figure 15. Phase A current; PWM supply, speed 1000 rpm

5. SIMULATION OF BPM MOTOR NO LOAD STARTUP

Another objective of the paper is to analyze the electromagnetic torque ripples during the no-load motor startup in case of six switches supply (section 5.2). This application supposes the coupling of the electromagnetic field equation (1) with the kinematics equation of the motor:

$$J\ddot{\theta} = T_e - T_r \quad (2)$$

where $J = 0.001 \text{ kgm}^2$ is the moment of inertia of the rotor, θ is the rotor angular position, $\ddot{\theta}$ is the angular acceleration, T_r is the resistive torque and T_e is the electromagnetic torque.

After the start-up transient regime of the motor that lasts approximately 3 s, the motor reaches the steady state at a rotation speed of roughly 4190 rpm, Fig. 16.

The electromagnetic torque shown in Fig. 17 increases abruptly during the motor start-up and decreases to a small steady-state value (peak-to-peak value of 0.28 Nm) that is characteristic to the no-load operation of the studied BPM motor.

In Fig. 18 is presented the time variation of phase current during the motor start-up. The phase current waveform in this application is characterized, as expected, by variable frequency that is correlated with the rotor position.

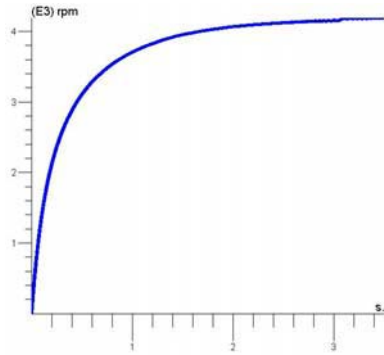


Figure 16. Time variation of speed during the no-load startup

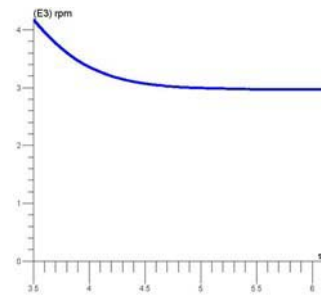


Figure 19. Time variation of the speed when the motor is loaded

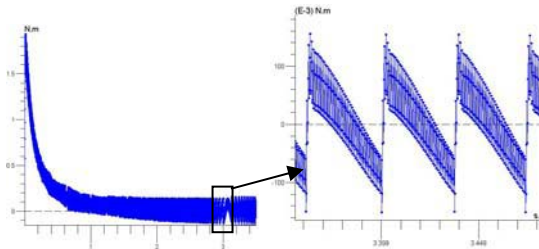


Figure 17. Time variation of the electromagnetic torque during the no-load startup

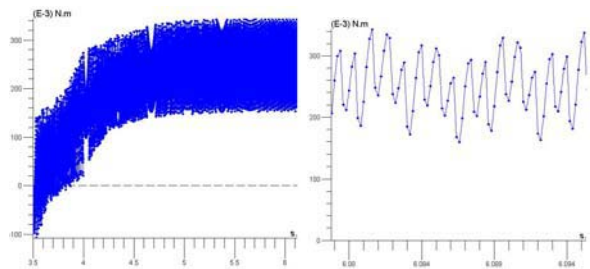


Figure 20. Time variation of the electromagnetic torque when the motor is loaded

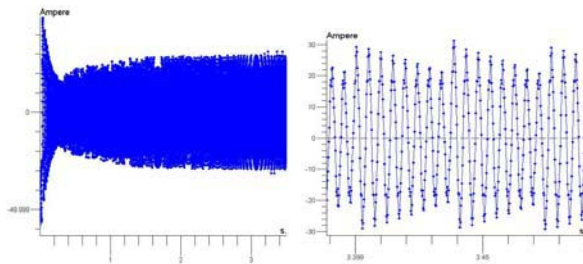


Figure 18. The time variation of the phase A current during the no-load startup

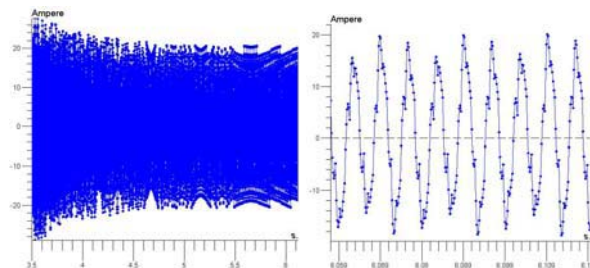


Figure 21. Time variation of the phase A current when the motor is loaded

6. DYNAMIC ANSWER OF BPM MOTOR AFTER APPLYING A LOAD TORQUE

The last studied case is dedicated to the transient regime of the motor after applying a load torque, $T_r = 0.25$ Nm. The initial state of the motor related to rotor speed and magnetic state in this case is the final state of the motor of the previous case (no-load steady state).

By studying the numerical results we can notice an important rotor speed decrease from no-load to load motor operation, from 4190 rpm to 2969 rpm, Fig. 19.

The oscillations of the electromagnetic torque in case of loaded motor are presented in Fig. 20. The corresponding phase current time variations during the studied transient regime of the BPM motor are presented in Fig. 21.

7. CONCLUSIONS

The finite element based analysis provides useful results for the designers of high performance BPM motor. The reduction of electromagnetic torque oscillations, a main source of vibration and acoustic noise, can be obtained by using a suitable command strategy for the motor. This study proves that the circuit command based on three switches entails large electromagnetic torque ripples with respect to the mean value, unsuitable for smooth torque applications. The six-switch circuit gives better results than the first arrangement, but the best arrangement was proved to be the command with PWM voltage inverter and the sine-wave phase

currents supply. In this last case, still smaller electromagnetic torque oscillations can be obtained by a minimization of the cogging torque ripples.

8. REFERENCES

- [1] T.J.E. Miller and J.R. Hendershot Jr., *Design of Brushless Permanent-Magnet Motors*, Magna physics publishing and Clarendon press, Oxford, 1994.
- [2] R. Carlson, M. Lajoie-Mazenc, J.C. dos S. Fagundes, *Analysis of Torque Ripple Due to Phase Commutation in Brushless DC Machines*", IEEE Transactions on Industry Applications, Vol. 28, No. 3, May/June 1992.
- [3] S. Brisset and P. Brochet, *Numerical simulation of the transients of a switched reluctance motor using an electronic-magnetic-mechanical coupled finite element model*, International Conference on Electric Machines (ICEM) 1994, pp. 402-406, September 1994.
- [4] G. Manot, Y. Lefevre, H. Piquet, *Integration of Feed Back Control in a Field Circuit Coupled Model*, International Symposium on Electromagnetic Fields in Electrical Engineering (ISEF) 2001.
- [5] T. Tudorache, V. Fireteanu, *Numerical analysis of DC brushless motors*, International Symposium ATEE 2002, Romania.
- [6] S.X. Chen, T.S. Low, *Analysis of Spindle Motor Performance Sensitivity to Excitation Schemes*, IEEE Transactions on Magnetics, Vol. 34, No. 2, March 1998.
- [7] S.X. Chen, T.S. Low, H. Lin, Z.J. Liu, *Design Trends of Spindle Motors for High Performance Hard Disk Drives*, in IEEE Transactions on Magnetics, Vol. 32, No. 5, September 1998.